

# X-ray diffraction from chiral molecules with twisted beams

Akilesh Venkatesh,<sup>1,\*</sup> Phay Ho,<sup>1</sup> and Jérémy R. Rouxel<sup>1,†</sup>

<sup>1</sup>*Chemical Sciences and Engineering, Argonne National Laboratory, Lemont, Illinois 60439, USA*

(Dated: March 2, 2026)

Structured x-rays carrying an orbital angular momentum break spatial inversion symmetry and have been proposed as a means to probe chirality. We theoretically investigate twisted non-resonant x-ray diffraction from chiral molecules and demonstrate that no dichroic signal can arise from randomly oriented molecules, irrespective of the beam spatial profile. However, a dichroic response is found to emerge if the molecule is oriented. Our results establish the beam and sample conditions for which a measurable dichroic scattering signal survives axial and focal averaging.

Chirality, the non-superimposability of an object and its mirror image, is a structural property that plays an important role in biochemistry [1], stereochemistry [1] and asymmetric catalysis [2]. Determining absolute configuration and enantiomeric excess is therefore essential. Conventional chiroptical techniques rely on the spin angular momentum (SAM) of light, i.e. its polarization [3, 4], and provide enantiomeric sensitivity in isotropic ensembles, yet they rarely yield direct atomic-scale structural information.

Standard x-ray diffraction (XRD) as a structural probe is insensitive to inversion-symmetry breaking, irrespective of whether the sample is crystalline [5]. For linear non-resonant elastic x-ray scattering, polarization only enters as the Lorentz-polarization prefactor [6] and does not couple to the scalar charge density. This results in Friedel's law: diffraction amplitudes at  $\pm\mathbf{q}$  momentum transfer are equal [5, 7], so enantiomers cannot be distinguished and their absolute configuration cannot be determined [8]. Close to an electronic resonance, structure factors acquire imaginary components and Bijvoet pairs differ in amplitude. This Bijvoet difference, together with anomalous dispersion, has been used for absolute structure determination [5, 9] in crystals.

The increasing availability of spatially structured x-rays enables new characterization methods [10] with x-rays carrying an Orbital Angular Momentum (OAM) attracting particular interest [11–16]. In addition to their SAM, these beams, also known as twisted or vortex beams, possess a spatially structured wavefront that has a topological charge [17, 18]. This usually manifests as a rotating phase in the field components (see Fig. 1). Twisted beams have been widely exploited in the optical domain [19, 20] and are emerging in x-ray applications including ptychography [21] and spectroscopy [22].

Since the OAM light-matter interaction provides a field pseudoscalar [23], it opens new routes to probe chirality-sensitive processes. Advantageously, OAM beams with its large set of controllable parameters offers additional paths for signal optimization. While twisted x-ray diffraction from chiral nanocrystals have been proposed [24], it remains unclear whether such effects persist in x-ray

diffraction from isotropic chiral media.

In the paraxial limit, the twisted wavefront and polarization decouple, and symmetry arguments enforce Friedel's law for ground state molecules. Yong *et al.* [25] have shown that time-resolved x-ray scattering from a single photoexcited molecule at the OAM beam center can exhibit a dichroic response, interpreted as a signature of conical-intersection passage, with related extensions to electron-vortex scattering [26]. Molecular chirality measurements in liquids and gases are inherently ensemble averaged. Single-molecule x-ray diffraction, which can avoid such averaging, remains experimentally challenging [27, 28]. This raises the question on whether the increased field gradients of tightly focused beams can reveal chiral structures under rotational and focal averaging. In this regime which lies beyond the paraxial approximation, the OAM and SAM are coupled and only the total angular momentum is well defined.

In this Letter, we establish under which conditions a chirality-sensitive dichroic signal can exist under nonresonant elastic scattering. We first prove using an irreducible expansion of the charge density that randomly oriented molecules cannot yield a difference signal between enantiomers. We then demonstrate through simulations that a non-vanishing dichroic signal can arise in the case of a single oriented molecule. We determine the conditions under which a dichroic scattering response can arise in an ensemble of chiral molecules, and show that these conditions are more restrictive than previously anticipated due to focal averaging effects and ensemble response. Atomic units are used throughout unless stated otherwise.

*X-ray diffraction with structured light*– For a monochromatic incident field of photon energy  $\omega_{\text{in}}$ , the vector potential is written as,  $A_{\text{in}}(\mathbf{r}, t) = A(\mathbf{r})e^{-i\omega_{\text{in}}t} + A^*(\mathbf{r})e^{i\omega_{\text{in}}t}$ , where  $\mathbf{r}$  and  $t$  denote position and time, respectively. The XRD signal  $s$  for a beam with an arbitrary spatial structure  $A(\mathbf{r})$  is given by [29]:

$$s(\mathbf{k}_s) \propto \int d\mathbf{r}d\mathbf{r}' \langle \sigma(\mathbf{r})\sigma^*(\mathbf{r}') \rangle_{\Omega} \times \mathbf{A}(\mathbf{r}) \cdot \boldsymbol{\epsilon}^* \mathbf{A}^*(\mathbf{r}') \cdot \boldsymbol{\epsilon} e^{-i\mathbf{k}_s \cdot (\mathbf{r}-\mathbf{r}')}, \quad (1)$$

where  $\sigma(\mathbf{r})$  is the matter total charge density,  $\boldsymbol{\epsilon}$  and  $\mathbf{k}_s$  are the scattered field polarization and wavevec-

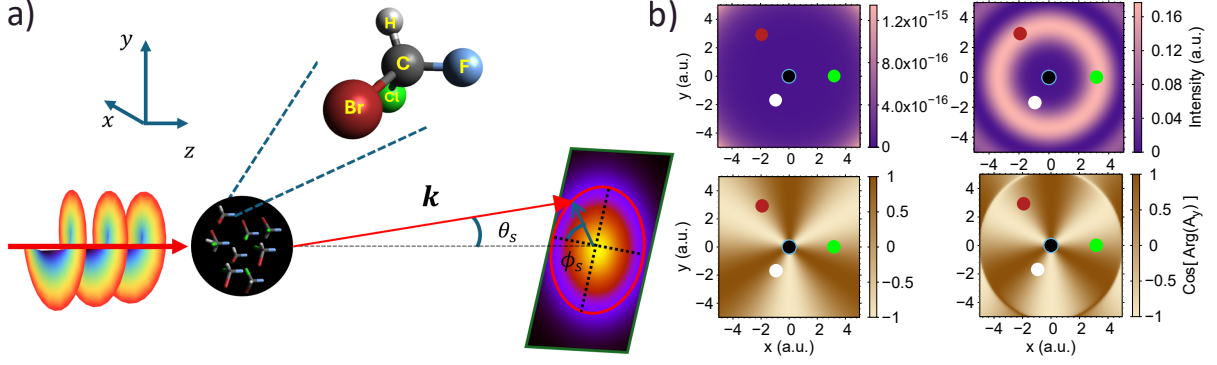


Figure 1: a) Scattering geometry for twisted x-ray diffraction from an axially oriented molecular ensemble. Inset: CHBrClF molecule (C–F along +z). b) Intensity (top) and phase profiles (bottom) in the  $z = 0$  plane for OAM beams with  $\omega_{\text{in}} = 9.25$  keV,  $m = +4$ ,  $\Lambda = +1$  and cone angles  $\theta_k = 0.1^\circ$  (left) and  $\theta_k = 30^\circ$  (right). Atomic positions shown (C: black; H: white; Br: maroon; Cl: green; F: blue) for a single oriented molecule with carbon at the beam center. Only the phase of  $A_y$  is shown. These two cases sample regimes with markedly different paraxial-approximation accuracy for the twisted field–matter interaction.

tor respectively.  $\langle \dots \rangle_\Omega$  indicates that a rotational averaging is carried over the matter.

First, we show that a randomly oriented molecule produces no dichroic signal, irrespective of the incident field's spatial structure. For this, we expand the matter correlation function in spherical harmonics and perform the rotational averaging:

$$\langle \sigma(\mathbf{r})\sigma^*(\mathbf{r}') \rangle_\Omega = \left\langle \sum_{lm} \sum_{l'm'} \sigma_{lm}(r)\sigma_{l'm'}^*(r') \times Y_{lm}(\hat{\mathbf{r}})Y_{l'm'}^*(\hat{\mathbf{r}}') \right\rangle_\Omega. \quad (2)$$

The two enantiomers of a chiral compound are transformed into each other by a parity operation. Thus, a signal capable of distinguishing them needs to be a pseudoscalar [4]. In many dichroic measurements, probing the difference signal between the  $\Delta$  and  $\Lambda$  enantiomers with a given incident field can be mimicked by making a differential measure with complementary chiral fields (usually switching polarization between left and right) on a given enantiomer. Outside the paraxial regime, switching the chirality of the twisted fields becomes non-trivial, therefore, we examine the difference yield between the enantiomers.

The differential matter correlation function is then given by:  $\langle \sigma^\Delta(\mathbf{r})\sigma^{\Delta,*}(\mathbf{r}') \rangle_\Omega - \langle \sigma^\Lambda(\mathbf{r})\sigma^{\Lambda,*}(\mathbf{r}') \rangle_\Omega$  where the parity operator  $P$  transforms  $\sigma^\Delta(\mathbf{r})$  into  $\sigma^\Lambda(\mathbf{r})$  up to a rotation. The spherical harmonics transform by parity as follows  $PY_{lm}(\Omega) = (-1)^l Y_{lm}(\Omega)$ . Using the spherical harmonics expansion and their parity properties,

we get:

$$\begin{aligned} & \langle \sigma^\Delta(\mathbf{r})\sigma^{\Delta,*}(\mathbf{r}') \rangle_\Omega - \langle \sigma^\Lambda(\mathbf{r})\sigma^{\Lambda,*}(\mathbf{r}') \rangle_\Omega = \\ & \sum_{lm} \sum_{l'm'} (1 - (-1)^{l+l'}) \sigma_{lm}(r)\sigma_{l'm'}^*(r') \langle Y_{lm}(\hat{\mathbf{r}})Y_{l'm'}^*(\hat{\mathbf{r}}') \rangle_\Omega \\ & = \sum_{lm} \sum_{l'm'} \sum_{m_1 m_2} (1 - (-1)^{l+l'}) \sigma_{lm}(r)\sigma_{l'm'}^*(r') \\ & \times \left( \int \frac{d\Omega}{8\pi^2} \mathcal{D}_{mm_1}^l(\Omega) \mathcal{D}_{m'm_2}^{l'}(\Omega) \right) Y_{lm_1}(\hat{\mathbf{r}}) Y_{l'm_2}^*(\hat{\mathbf{r}}') = 0. \end{aligned} \quad (3)$$

where  $\mathcal{D}_{mm'}^l(\Omega)$  are Wigner  $\mathcal{D}$  matrices and  $\Omega$  denotes the set of Euler angles. Orthogonality of the  $\mathcal{D}$  matrices enforces  $l = l'$ , hence  $(1 - (-1)^{l+l'}) = 0$ . Therefore, the elastic Thomson contribution to any dichroic scattering signal vanishes upon full rotational averaging. This cancellation depends only on the matter terms and is independent of the incident beam spatial profile.

To retain parity odd contributions, we consider oriented molecules, for which axial (cylindrical) averaging replaces full rotational averaging. For plane wave x-ray diffraction, similar to the Debye scattering equation for full rotational averaging, an analogous expression for oriented molecules was derived previously [30, 31]. The scaled scattering yield for a plane wave incident on a cylindrically averaged group of atoms is:

$$\frac{S(\mathbf{q})}{S_e} = \sum_{ij} f_i(q)f_j(q) \cos(q_z r_{ijz}) J_0 \left( r_{ijxy} \sqrt{q_x^2 + q_y^2} \right), \quad (4)$$

where  $r_{ijxy} = \sqrt{(r_{ix} - r_{jx})^2 + (r_{iy} - r_{jy})^2}$ ,  $r_{ijz} = |r_{iz} - r_{jz}|$ ,  $f_i(q)$  is the atomic structure factor of the  $i$ th atom,  $\mathbf{q} = \mathbf{k}_{\text{in}} - \mathbf{k}_s$ ,  $S(\mathbf{q})$  is the scattering yield, and  $S_e$  is the Thomson scattering yield from a free electron. The quantities  $\mathbf{k}_{\text{in}}$  and  $\mathbf{k}_s$  denote the incident photon momentum of the plane wave and the scattered photon momentum, respectively.

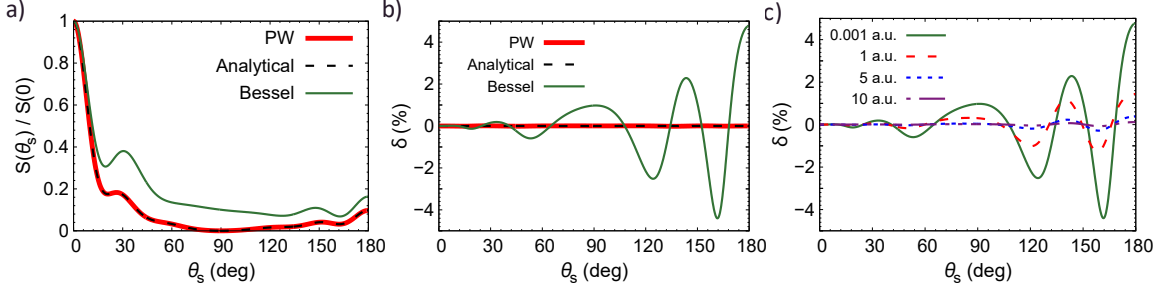


Figure 2: a) Scattering yields for a single molecule at the beam center ( $\sigma_b = 0.001$  a.u.) after axial averaging: linearly polarized plane wave (PW), Debye-scattering analog for axial averaging (Analytical), and OAM Bessel beam (Bessel) with  $\theta_k = 30^\circ$ ,  $m = 4$ , and  $\Lambda = 1$ . b) Dissymmetry factor  $\delta$  (percentage difference in yield) between enantiomers. c)  $\delta$  vs distance from beam center, revealing focal averaging effects.  $\phi_s = 90^\circ$  for all cases.

No closed-form expression exists for scattering of an OAM beam by an ensemble of randomly located, axially averaged molecules. In this work, we simulate the elastic x-ray response numerically using a monochromatic OAM Bessel beam [32, 33]. The spatial part  $\mathbf{A}(\mathbf{r})$  of the twisted Bessel field, from Böning et al. [32], is expressed as  $\mathbf{A}(\mathbf{r}) = \mathbf{g}(\rho, \phi) e^{ik_z z}$ . The position vector  $\mathbf{r}(\rho, \phi, z)$  is given in cylindrical coordinates where  $\rho$ ,  $\phi$  and  $z$  denote the radial, azimuthal and axial coordinate, respectively. The vector  $\mathbf{g}$  is defined as

$$g_x = \frac{1}{2} A_0 \sqrt{\frac{k_\perp}{4\pi}} \left\{ c_{-1} J_{m+1}(k_\perp \rho) e^{i(m+1)\phi} + c_{+1} J_{m-1}(k_\perp \rho) e^{i(m-1)\phi} \right\}, \quad (5)$$

$$g_y = \frac{1}{2i} A_0 \sqrt{\frac{k_\perp}{4\pi}} \left\{ c_{-1} J_{m+1}(k_\perp \rho) e^{i(m+1)\phi} - c_{+1} J_{m-1}(k_\perp \rho) e^{i(m-1)\phi} \right\}, \quad (6)$$

$$g_z = \frac{1}{2i} A_0 \sqrt{\frac{k_\perp}{2\pi}} c_0 J_m(k_\perp \rho) e^{im\phi}. \quad (7)$$

Here  $k_\perp = (\omega_{\text{in}}/c) \sin \theta_k$  and  $k_z = (\omega_{\text{in}}/c) \cos \theta_k$  are the perpendicular and parallel components of the linear momentum of the Bessel beam where  $c$  is the speed of light in vacuum and  $\theta_k$  is the OAM beam cone opening angle. The coefficients are  $c_{\pm 1} = (1 \pm \Lambda \cos \theta_k)/2$  and  $c_0 = \Lambda \sin \theta_k / \sqrt{2}$ . The quantities  $A_0$ ,  $J_m$ ,  $m$ , and  $\Lambda$  are the field amplitude, Bessel function of the first kind, projection of the total angular momentum along the propagation direction, and beam helicity, respectively. The cone angle  $\theta_k$  determines the radial spacing of the Bessel zeros and thus controls the beam's transverse size.

The above field  $\mathbf{A}(\mathbf{r})$  [Eqs. (5)-(7)] is an exact solution of the Helmholtz equation and an eigen-vector of the total angular momentum projection along beam-axis  $J_z$  with eigenvalue  $m$  [33]. Although the intensity profile for  $|m|$  and  $-|m|$  are

not identical, in the paraxial limit the intensity profiles for  $|m|$  and  $2 - |m|$  become approximately equal and the fields become approximately complementary (see SM). In that paraxial limit, SAM and OAM decouple to yield well-defined corresponding values  $\Lambda$  and  $(m - \Lambda)$  respectively and the component  $A_z(\mathbf{r}) \approx 0$ . For  $\theta_k \rightarrow 0$ , with  $m = \pm 1$  and  $\Lambda = \mp 1$ , the field reduces to circularly polarized field.

*Computational approach*— We investigate twisted x-ray diffraction from chiral molecules using the independent atom model model. We retain the field's spatial variation across atomic centers while neglecting intra-atomic field variations. For a single molecule with scattered photon momentum  $\mathbf{k}_s$  and polarization  $\boldsymbol{\epsilon}$ , the scattering amplitude is (see SM)

$$F_1 = \sum_a^{n_a} f_a(\mathbf{Q}) e^{i\mathbf{Q} \cdot \mathbf{R}_a} \boldsymbol{\epsilon}^* \cdot \mathbf{g}(\rho_a, \phi_a). \quad (8)$$

where  $\mathbf{Q} = \mathbf{k}_z - \mathbf{k}_s$  and  $\mathbf{k}_z = k_z \hat{z}$ . The quantities  $f_a(\mathbf{Q})$  and  $\mathbf{R}_a$  are the atomic form factor and position of the atom  $a$ , respectively.  $n_a$  denotes the number of atoms in a single molecule.

We simulate twisted x-ray diffraction on an archetypal chiral molecule, bromochlorofluoromethane (CHBrClF) with the C-F bond fixed along the  $z$ -direction (Fig. 1). We compute scattering for both a single molecule and for molecular ensembles. For the single molecule runs, we evaluate the scattering yield  $S = |F_1|^2$  for a uniform random axial rotation around the C-F bond in the interval  $[0, 2\pi]$  and for an impact parameter drawn from a zero-mean Gaussian distribution with rms  $\sigma_b$ . Then the scattering yield is averaged over a billion realizations. The parameter  $\sigma_b$  models focal-volume-limited interaction and tolerance in the impact parameter. For ensembles, the scattering yield is the absolute square of the coherent sum of individual molecular scattering amplitudes (each molecule generated as above). Ensemble results are averaged over 30 million realizations. All reported yields are summed over the two outgoing

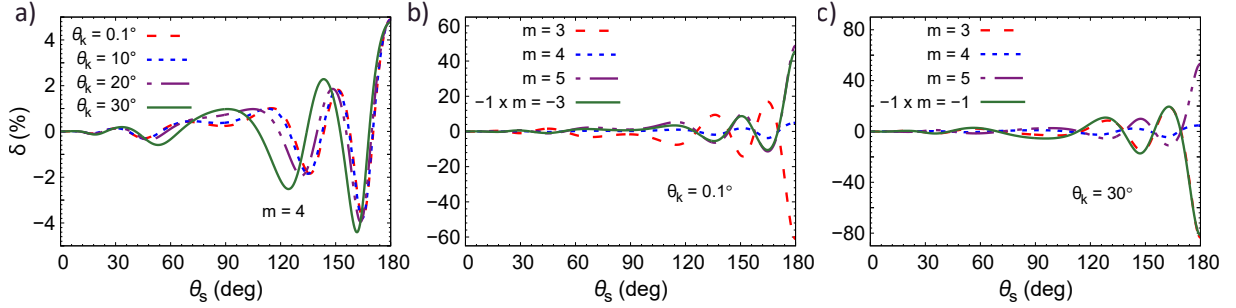


Figure 3: Dissymmetry factor  $\delta$  vs Bessel beam parameters. a)  $\theta_k$  dependence for fixed  $m = 4$ . b)  $m$ -dependence for  $\theta_k = 0.1^\circ$ . c)  $m$ -dependence for  $\theta_k = 30^\circ$ . In all cases,  $\Lambda = 1$ ,  $\phi_s = 90^\circ$ .

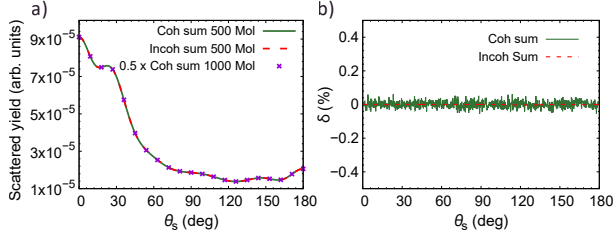


Figure 4: a) Scattering yields for ensembles of 500 and 1000 molecules. “Coh sum”:  $|\sum_i F_i|^2$ , “Incoh sum”:  $\sum_i |F_i|^2$ . b) Differential yield between enantiomers for the 500-molecule ensemble. The other parameters are identical to Fig. 2.

photon polarizations (i.e. the scattered photon polarization is not measured). Given the scattering yields  $S_\Delta$  and  $S_\Lambda$  for the  $\Delta$  and  $\Lambda$  enantiomers, respectively, the dissymmetry factor  $\delta$  is defined as

$$\delta = \frac{\langle S_\Delta \rangle - \langle S_\Lambda \rangle}{0.5(\langle S_\Delta \rangle + \langle S_\Lambda \rangle)} \times 100. \quad (9)$$

*Results and Discussion*— Fig. 2a shows the scattering yield of a single  $\Delta$  molecule located at the beam center. The plane-wave result (solid red curve, PW) is for a linearly polarized incident field for in-plane scattering ( $\phi_s = 90^\circ$ ). The yield obtained from the analytical expression in Eq. (4) is also displayed. Its agreement with our stochastic plane-wave simulation provides a benchmark. Notably, the plane-wave yield vanishes at  $\theta_s = 90^\circ$ , whereas the twisted yield does not. For a linearly polarized plane wave, the polarization factor  $|\epsilon \cdot \epsilon_{\text{in}}|^2$  vanishes at  $\theta_s = 90^\circ$  for in-plane scattering ( $\phi_s = 90^\circ$ ), which is not the case for the twisted Bessel field [Eq. (8)]. Furthermore, the plane-wave scattering yield depends on the azimuthal angle  $\phi_s$  due to this polarization factor and not due to the underlying molecular structure. In contrast, the twisted beam yields show no azimuthal angle dependence.

Fig. 2b shows the dissymmetry factor  $\delta$  [Eq. (9)]. For conventional plane wave x-ray diffraction,  $\delta$  vanishes for all scattering angles, even for a perfectly oriented chiral molecule. In contrast, a twisted x-ray field yields a clear non-zero dichroic

signal when the molecule is centered in the beam. The twisted field introduces intensity and phase gradients across the molecule (Fig. 1b), leading to different phases and probabilities for the scattered wave from each atom in the molecule. The resulting interference pattern remains chiral-sensitive after axial averaging. The dissymmetry factor is zero in the forward direction and maximal in backward elastic scattering. In the paraxial limit, the forward cancellation can be shown analytically: complementary twisted beams produce equal and opposite contributions from atomic pairs (see SM). Our result demonstrates that this vanishing persists well beyond the paraxial regime, confirms trends implicit in Ref. [24], and clarifies their origin.

Fig. 2c shows the dependence of the  $\delta$  on the rms position  $\sigma_b$ . Relaxing the restriction that the molecule is at the beam center introduces both axial and positional averaging, leading to a rapid suppression of the dichroic signal. As the molecule is located further from the beam center, the field gradient across its atoms decreases. For large displacements, the molecule effectively experiences a plane wave, whose dichroic response does not survive axial averaging. Focal averaging plays a decisive role in the survival of dichroism in disordered systems illuminated by twisted beams.

Fig. 3 reveals the dependence of  $\delta$  on the Bessel beam parameters (topological charge  $m$  and cone angle  $\theta_k$ ) for a molecule near the beam center. Increasing  $\theta_k$  (Fig. 3a) causes both intensity and phase gradients across the molecules, yielding a moderate increase in  $\delta$ .

An intuitive argument can be made for the non-monotonic dependence of the dichroic signal on  $m$  (see (Fig. 3b) as a function of the molecular geometry: for the chosen system (central chirality oriented along one of its bonds), the atoms are approximately organized in a three-fold symmetry, which matches the periodicity of the phase rotation of an  $m = 4$  beam (see Fig. 1b). Thus, each atom experiences almost the same relative phase of the OAM beam and the dichroic signal is strongly reduced. Alternatively, other  $m$  values that cause larger phase gradients between different atomics

sites across the molecules will increase the effect of the twisted wavefronts on the scattering signal. Since beams with  $J_z$  values  $|m|$  and  $-|m|$  have different intensity profiles, their dichroic responses are not identical. However, in the paraxial approximation, replacing  $m$  by its complementary value  $2-|m|$  approximately mimics the effect on the scattering yield from mirror inversion of the molecule. The calculations (Figs. 3b & 3c) show that this approximation is most accurate for backward elastic scattering and that  $\delta$  is maximized there.

Fig. 4 considers an ensemble with rms position  $\sigma_b \approx 53$  nm (1000 a.u.), comparable to achievable x-ray focal size. Fig. 4a shows the scattering yield for ensembles of 500 and 1000 molecules respectively, which corresponds to an ideal gas at 300 K with pressures of about 0.14 and 0.28 atm. The coherent sum is  $|\sum_i F_i|^2$ , whereas the incoherent sum is  $\sum_i |F_i|^2$ . Note that  $|F_1|^2$  [Eq. (8)] already includes coherent (intra-molecular) interference among atomic amplitudes, which generates the dichroism. The agreement between coherent and incoherent sums indicates the absence of inter-molecular interference upon ensemble averaging. The random positions and random axial orientations of the molecules ensure that there exists no fixed phase difference between the incident fields experienced by two molecules. This gives rise to scattered fields from two molecules with no fixed phase difference. Consequently, the total twisted scattered yield scales linearly with number of molecules, analogous to conventional XRD.

Fig. 4b shows that the ensemble dissymmetry factor  $\delta$  effectively vanishes for all scattering angles. The dichroic signal arises predominantly from molecules near the beam axis. Molecules far from the center effectively experience a locally plane-wave incident field and do not encounter the twisted spatial structure. The limited number of molecules at the center, together with the reduced on-axis intensity, render the difference yield to total yield ratio negligible. Small deviations from zero reflect finite statistical sampling. The dissymmetry factor  $\delta$  computed from only the incoherent sum is closer to zero than that from the coherent sum which exhibits small high-frequency oscillations, indicating that the dominant statistical noise originates from intermolecular interference terms which do not cancel for a finite number of realizations. These results demonstrate that focal averaging, i.e. the inability to confine molecules close to the beam axis, critically suppresses chiral sensitivity in disordered ensembles. Finally, although the twisted scattering yields can depend on the detected photon polarization, the dichroic signal still vanishes under focal averaging, even with polarization sensitivity.

*Conclusion and Summary*– In this Letter, we theoretically investigated x-ray scattering with twisted Bessel beams to probe chiral molecules with simulations presented for a simple chiral

molecular system CHBrClF. We prove that irrespective of the properties of the incident beam, upon full rotational averaging, there exists no difference in the nonresonant elastic scattering signal between enantiomers. However, for an oriented molecule, there exists a difference signal between the enantiomers which depends on the parameters of the Bessel beam. Scattering calculations from an ensemble of oriented chiral molecules highlight the pivotal role focal averaging effects can play in diminishing an observable dichroic signal independent from any temperature effects on orientation. The results also strongly suggest that twisted x-ray scattering is likely to be effective in probing chirality in crystalline samples where these effects are reduced.

*Acknowledgements*– AV benefited from prior discussions and early modelling of twisted Bessel beams with F. Robicheaux. This work was supported by the U.S. Department of Energy, Office of Basic Energy Sciences, Division of Chemical Sciences, Geosciences, and Biosciences through Argonne National Laboratory. Argonne is a U.S. Department of Energy laboratory managed by UChicago Argonne, LLC, under Contract No. DE-AC02-06CH11357. We gratefully acknowledge the computing resources provided on Improv, a high-performance computing cluster operated by the Laboratory Computing Resource Center at Argonne National Laboratory.

*Data availability*– The data presented in the figures will be available upon reasonable request.

---

\* akilesh.venkatesh1[at]gmail[dot]com

† jrouxel@anl.gov

- [1] Joseph Gal. Molecular chirality in chemistry and biology: Historical milestones. *Helvetica Chimica Acta*, 96(9):1617–1657, 2013.
- [2] Patrick J Walsh and Marisa C Kozlowski. *Fundamentals of asymmetric catalysis*. University Science Books, 2009.
- [3] Nina Berova, Koji Nakanishi, and Robert W Woody. *Circular dichroism: principles and applications*. John Wiley & Sons, 2000.
- [4] Laurence D Barron. *Molecular light scattering and optical activity*. Cambridge University Press, 2009.
- [5] Simon Parsons. Determination of absolute configuration using x-ray diffraction. *Tetrahedron: Asymmetry*, 28(10):1304–1313, 2017.
- [6] Jens Als-Nielsen and Des McMorrow. *Elements of modern X-ray physics*. John Wiley & Sons, 2011.
- [7] Georges Friedel. Sur les symétries cristallines que peut révéler la diffraction des rayons röntgen. *CR Acad. Sci. Paris*, 157:1533–1536, 1913.
- [8] Rob WW Hooft, Leo H Straver, and Anthony L Spek. Determination of absolute structure using bayesian statistics on bijvoet differences. *Journal of Applied Crystallography*, 41(1):96–103, 2008.
- [9] HD Flack and G Bernardinelli. The use of x-ray crystallography to determine absolute configuration. *Chirality: The Pharmacological, Biological,*

- and *Chemical Consequences of Molecular Asymmetry*, 20(5):681–690, 2008.
- [10] Andrew Forbes, Michael De Oliveira, and Mark R Dennis. Structured light. *Nature Photonics*, 15(4):253–262, 2021.
- [11] Shigemi Sasaki and Ian McNulty. Proposal for generating brilliant x-ray beams carrying orbital angular momentum. *Physical review letters*, 100(12):124801, 2008.
- [12] Lyuzhou Ye, Jérémy R Rouxel, Shahaf Asban, Benedikt Rösner, and Shaul Mukamel. Probing molecular chirality by orbital-angular-momentum-carrying x-ray pulses. *Journal of chemical theory and computation*, 15(7):4180–4186, 2019.
- [13] Nanshun Huang and Haixiao Deng. Generating x-rays with orbital angular momentum in a free-electron laser oscillator. *Optica*, 8(7):1020–1023, 2021.
- [14] Justin S Woods, Xiaoqian M Chen, Rajesh V Chopdekar, Barry Farmer, Claudio Mazzoli, Roland Koch, Anton S Tremsin, Wen Hu, Andreas Scholl, Steve Kevan, et al. Switchable x-ray orbital angular momentum from an artificial spin ice. *Physical review letters*, 126(11):117201, 2021.
- [15] Jiawei Yan and Gianluca Geloni. Self-seeded free-electron lasers with orbital angular momentum. *Advanced Photonics Nexus*, 2(3):036001–036001, 2023.
- [16] Margaret R McCarter, Lance E De Long, J Todd Hastings, and Sujoy Roy. Generation and applications of x-ray and extreme ultraviolet beams carrying orbital angular momentum. *Journal of Physics: Condensed Matter*, 36(42):423003, 2024.
- [17] L Allen, MJ Padgett, and M Babiker. Iv the orbital angular momentum of light. In *Progress in optics*, volume 39, pages 291–372. Elsevier, 1999.
- [18] Juan P Torres and Lluís Torner. *Twisted photons: applications of light with orbital angular momentum*. John Wiley & Sons, 2011.
- [19] Yijie Shen, Xuejiao Wang, Zhenwei Xie, Changjun Min, Xing Fu, Qiang Liu, Mali Gong, and Xiaocong Yuan. Optical vortices 30 years on: Oam manipulation from topological charge to multiple singularities. *Light: Science & Applications*, 8(1):90, 2019.
- [20] Nimish P Nazirkar, Viet Tran, Pascal Bassène, Atoumane Ndiaye, Julie Barringer, Jie Jiang, Wonsuk Cha, Ross Harder, Jian Shi, Moussa N’Gom, et al. Manipulating ferroelectric topological polar structures with twisted light. *Advanced Materials*, 37(33):2415231, 2025.
- [21] Matteo Pancaldi, Francesco Guzzi, Charles S Bevis, Michele Manfreda, Jonathan Barolak, Stefano Bonetti, Iuliia Bykova, Dario De Angelis, Giovanni De Ninno, Mauro Fanciulli, et al. High-resolution ptychographic imaging at a seeded free-electron laser source using oam beams. *Optica*, 11(3):403–411, 2024.
- [22] Jérémy R Rouxel, Benedikt Rösner, Dmitry Karpov, Camila Bacellar, Giulia F Mancini, Francesco Zinna, Dominik Kinschel, Oliviero Cannelli, Malte Oppermann, Cris Svetina, et al. Hard x-ray helical dichroism of disordered molecular media. *Nature Photonics*, 16(8):570–574, 2022.
- [23] Dale Green and Kayn A Forbes. Optical chirality of vortex beams at the nanoscale. *Nanoscale*, 15(2):540–552, 2023.
- [24] Nimish P Nazirkar, Xiaowen Shi, Jian Shi, Moussa N’Gom, and Edwin Fohtung. Coherent diffractive imaging with twisted x-rays: Principles, applications, and outlook. *Applied Physics Reviews*, 11(2), 2024.
- [25] Haiwang Yong, Jérémy R Rouxel, Daniel Keefer, and Shaul Mukamel. Direct monitoring of conical intersection passage via electronic coherences in twisted x-ray diffraction. *Physical Review Letters*, 129(10):103001, 2022.
- [26] Haowei Wu and Haiwang Yong. Diffractive imaging of transient electronic coherences in molecules with electron vortices. *Physical Review Letters*, 134(7):073001, 2025.
- [27] Richard Neutze, Remco Wouts, David Van der Spoel, Edgar Weckert, and Janos Hajdu. Potential for biomolecular imaging with femtosecond x-ray pulses. *Nature*, 406(6797):752–757, 2000.
- [28] Henry N Chapman. X-ray free-electron lasers for the structure and dynamics of macromolecules. *Annual review of biochemistry*, 88(1):35–58, 2019.
- [29] Kochise Bennett, Markus Kowalewski, Jérémy R Rouxel, and Shaul Mukamel. Monitoring molecular nonadiabatic dynamics with femtosecond x-ray diffraction. *Proceedings of the National Academy of Sciences*, 115(26):6538–6547, 2018.
- [30] Hideyo Inouye, Paul E Fraser, and Daniel A Kirschner. Structure of beta-crystallite assemblies formed by alzheimer beta-amyloid protein analogues: analysis by x-ray diffraction. *Biophysical journal*, 64(2):502–519, 1993.
- [31] AE Ross, DG McCulloch, and DR McKenzie. Extending the debye scattering equation for diffraction from a cylindrically averaged group of atoms: detecting molecular orientation at an interface. *Foundations of Crystallography*, 76(4):468–473, 2020.
- [32] Birger Böning, Willi Paufler, and Stephan Fritzsche. Above-threshold ionization by few-cycle bessel pulses carrying orbital angular momentum. *Physical Review A*, 98(2):023407, 2018.
- [33] Oliver Matula, Armen G Hayrapetyan, Valeriy G Serbo, Andrey Surzhykov, and Stephan Fritzsche. Atomic ionization of hydrogen-like ions by twisted photons: angular distribution of emitted electrons. *Journal of Physics B: Atomic, Molecular and Optical Physics*, 46(20):205002, 2013.